International Journal of Nanoscience
Vol. 4, No. 3 (2005) 269–286

World Scientific
www.worldscientific.com

ION BEAM LITHOGRAPHY AND NANOFABRICATION: A REVIEW

F. WATT*, A. A. BETTIOL, J. A. VAN KAN, E. J. TEO and M. B. H. BREESE

Centre for Ion Beam Applications (CIBA), Physics Department
National University of Singapore, Singapore 117542
**phywattf@nus.edu.sg*

Received 17 December 2004

To overcome the diffraction constraints of traditional optical lithography, the next generation lithographies (NGLs) will utilize any one or more of EUV (extreme ultraviolet), X-ray, electron or ion beam technologies to produce sub-100 nm features. Perhaps the most under-developed and under-rated is the utilization of ions for lithographic purposes. All three ion beam techniques, FIB (Focused Ion Beam), Proton Beam Writing (*p*-beam writing) and Ion Projection Lithography (IPL) have now breached the technologically difficult 100 nm barrier, and are now capable of fabricating structures at the nanoscale. FIB, *p*-beam writing and IPL have the flexibility and potential to become leading contenders as NGLs.

The three ion beam techniques have widely different attributes, and as such have their own strengths, niche areas and application areas. The physical principles underlying ion beam interactions with materials are described, together with a comparison with other lithographic techniques (electron beam writing and EUV/X-ray lithography). IPL follows the traditional lines of lithography, utilizing large area masks through which a pattern is replicated in resist material which can be used to modify the near-surface properties. In IPL, the complete absence of diffraction effects coupled with ability to tailor the depth of ion penetration to suit the resist thickness or the depth of modification are prime characteristics of this technique, as is the ability to pattern a large area in a single brief irradiation exposure without any wet processing steps. *p*-beam writing and FIB are direct write (maskless) processes, which for a long time have been considered too slow for mass production. However, these two techniques may have some distinct advantages when used in combination with nanoimprinting and pattern transfer. FIB can produce master stamps in any material, and *p*-beam writing is ideal for producing three-dimensional high-aspect ratio metallic stamps of precise geometry. The transfer of large scale patterns using nanoimprinting represents a technique of high potential for the mass production of a new generation of high area, high density, low dimensional structures. Finally a cross section of applications are chosen to demonstrate the potential of these new generation ion beam nanolithographies.

Keywords: Focused ion beam; proton beam writing; ion projection lithography; ion beam lithography; nanofabrication.

*Corresponding author.

1. Introduction

Next generation lithographies (NGLs) are being actively developed to take over from the highly successful optical lithography. As feature sizes shrink well below 100 nm, several key challenges for optical lithography have arisen that make it increasingly difficult to remain in step with Moore's Law.[1] The 2002 International Technology Roadmap for Semiconductors[2] lists optical mask fabrication, together with yield, cost and quality of calcium fluoride lenses amongst the difficult challenges that need to be overcome in the next few years as semiconductor manufacturers move towards the 65 nm node. Slower than expected technical development has recently prompted Intel to skip the 157 nm generation of lithography in favor of EUV. Other key challenges include the development of resist materials for 157 nm lithography and beyond, coupled with the escalating cost of lithography tools. Each of the potential NGLs (which include EUV, X-ray, electron and ion lithographies) are based on fundamentally different physical principles (see Box 1) implying that each lithographic technique will exhibit unique properties, and only in the next few years will we know which will be adopted as the prevailing technology of the future. Although the two front runners for the next generation lithographies are EUV and Electron Projection Lithography (EPL), increasing attention is being paid to the high potential of ion beam lithography as a serious alternative contender.

Box 1. The different physical interactions of fast light ions, slow heavy ions, electrons and electromagnetic radiation (EUV and X-rays) with matter.

***Fast light ions*:** The primary interaction is that of ion/electron collisions, and therefore many thousands of collisions will occur before an ion comes to rest. Trajectories and energy loss profiles can be accurately simulated by means of Monte Carlo calculations (for example using the computer code SRIM[3]). As an example, for 2 MeV protons, the penetration depth in PMMA is 60.8 μm, with a 2 μm lateral broadening of the beam at the end of range. However, the beam broadening is only 3 nm at 1 μm depth in the PMMA and 30 nm at 5 μm so beam broadening of fast protons in a thin resist layer is minimal.

***Slow heavy ions*:** The primary mechanism is that of high momentum transfer between the slow moving incident heavy ions and the atoms on the surface of the material. The surface atoms are re-arranged, resulting in chemical and structural changes as well as sputtering of atomic and molecular species from the surface. The sputtering mechanism can be calculated using Monte Carlo techniques (e.g., SRIM[3]) to show that the sputtering rate for a 30 keV gallium ion is around 1–10 atoms per incident ion for a wide variety of materials.

***Electrons*:** The primary interaction is that of electron/electron collisions, and this results in large angle multiple scattering of the electron beam leading to the classic "pear shaped" ionization volume around the point of entry into the material. The

(*Continued*)

Box 1. (*Continued*)

trajectories can be simulated using Monte Carlo techniques such as Casino[4]: As an example, 50 keV electrons penetrate up to depth of 40 μm in PMMA, with a 20 μm spread in the beam. Sub-100 nm e-beam writing therefore can only be realized in very thin resist layers, and high aspect ratio structures fabricated using additional steps e.g., reactive ion etching.

***EUV and X-rays*:** Photons react with the atomic electrons through the photoelectric effect, where the incident photon is completely absorbed by an atomic electron leading to the ejection of the electron from the atom, and by Rayleigh (elastic) scattering where the photon is scattered without an energy change. These processes can be simulated by computer software (see for example GEANT4[5]). A photon beam penetrating a resist material therefore does not have a defined range, and has an exponentially decreasing dose distribution with penetration depth.

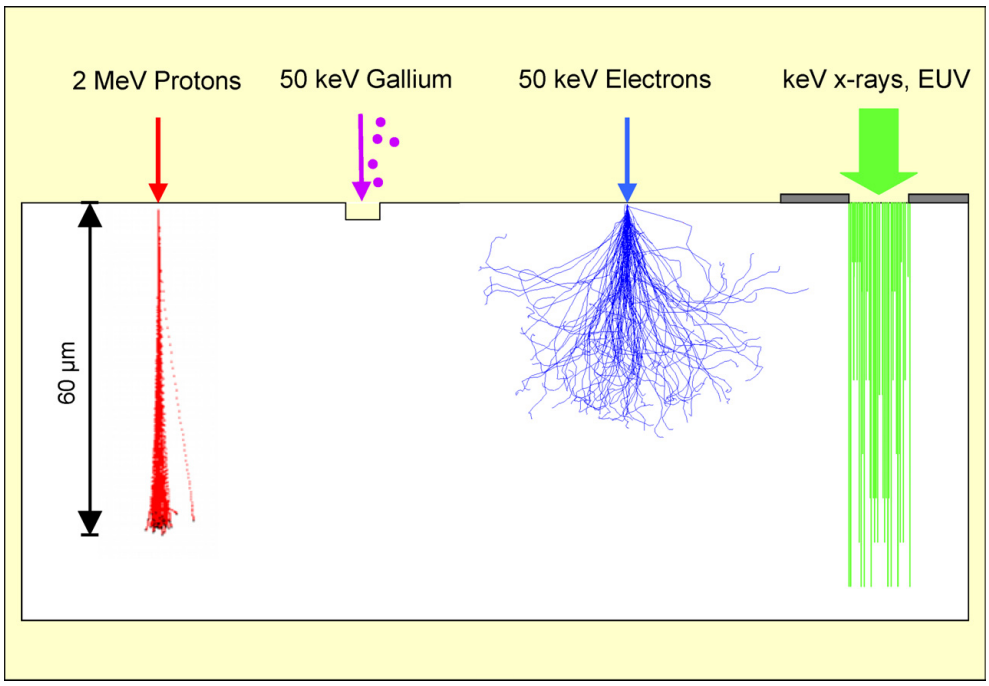

There are currently three separate and distinct ion beam processes capable of fabricating structures at the sub-100 nm level: The focused ion beam (FIB) technique where a slow focused heavy ion beam (with energies typically around 30 keV) is written over a surface to create a pattern through modification, deposition or sputtering; proton beam writing, where fast (typically MeV) protons are used to direct-write deep precise 3D patterns into resist, and ion projection lithography (IPL), where medium energy ions (typically 100 keV) are projected through a patterned mask for rapid fabrication. Schematic diagrams of the operating principles of these three processes are shown in Fig. 1 (Focused Ion Beam), Fig. 2 (p-beam writing) and Fig. 3 (Ion Projection Lithography). These three ion beam techniques are not only capable of fabricating structures below the technologically important

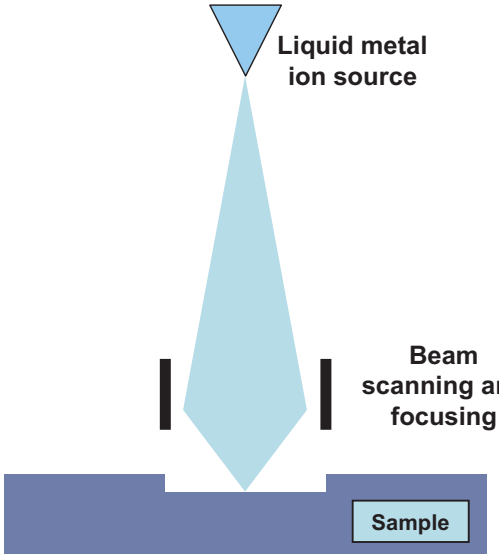

Fig. 1. A schematic diagram of a FIB system. The ion beam (usually gallium) is generated from a liquid metal source (LMIS) and the Ga^+ ions are focused down a column, similar in principle to that of a scanning electron microscope, on to the substrate. For focused ion beam chemical vapor deposition (FIBCVD), provision is usually made for a gas nozzle assembly next to the sample so as to provide a flow of gas molecules to the sample surface during irradiation.

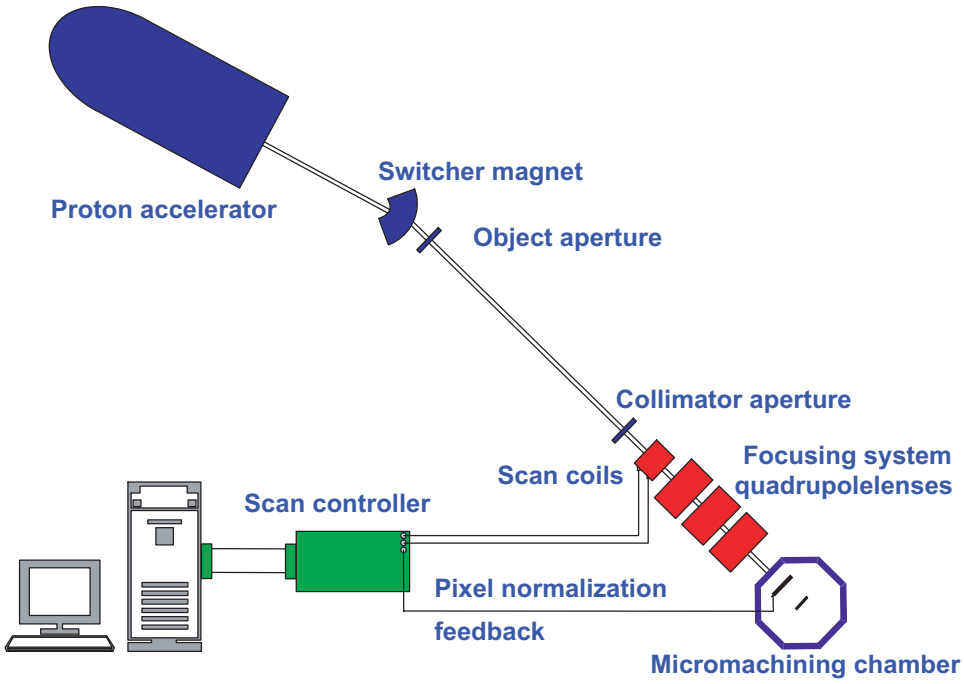

Fig. 2. A typical set-up for a proton beam writer. MeV protons are produced in a proton accelerator, and a demagnified image of the beam transmitted through an object aperture is focused onto the substrate material (resist) by means of a series of strong focusing magnetic quadrupole lenses (e.g., quadrupole triplet). Beam scanning takes place using magnetic or electrostatic deflection before the focusing lenses, and is driven by a feedback signal derived from the proton interactions with the resist. This feedback mechanism ensures a constant beam exposure per pixel as the beam is scanned across the resist, resulting in high quality structures.

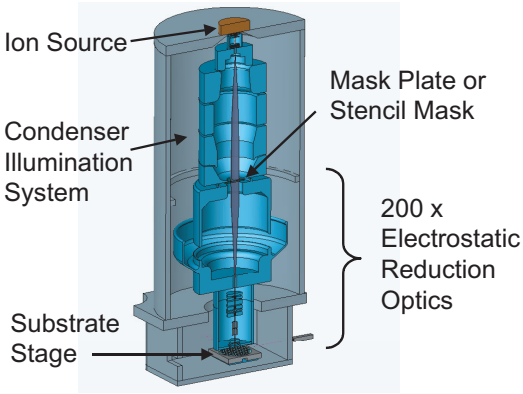

Fig. 3. Schematic diagram of the Ion Projection Lithography system (PROFIB) developed at IMS (reproduced with kind permission of H. Loeschner). The multi-cusp ion source produces a He, Ar or Xe ion beam which is passed through a stencil mask, and the ion-optical system with a 200x reduction projects the highly parallel transmitted ions on to the substrate.

100 nm barrier (see Fig. 4), but all three processes have highly appropriate and complementary application areas.

1.1. *Physical properties of ion beams*

Lithography using ion beams has several unique characteristics, primarily due to the physical nature of the ion (a charged particle is at least three orders of magnitude heavier than the electron). For slow heavy ions (e.g., 30 keV Ga^+), the interaction process is that of altering the surface structure of a material, modifying surface chemistry, and removing atoms from the surface through sputtering. In contrast, the primary interaction of fast lighter ions (e.g., 100 keV–3 MeV protons) is that of deep penetration into the material, with a minimal amount of surface disruption. For both light and heavy ions, diffraction effects are not an issue (the wavelength of a 100-keV proton is around 10^{-4} nm). For fast lighter ions, the interaction with matter provides some interesting properties: (a) The ion beam travels in a straight line apart from some end of range broadening. This offers a considerable advantage over e-beam writing for fabricating high aspect ratio 3D structures since a finely focused electron beam spreads rapidly as it enters the resist material (see Box 1). (b) The dose exposure as the ions penetrate the material is relatively constant (apart from an increase at the end of range). This feature offers an advantage over EUV or X-ray lithography, which exhibit an exponential reduction in dose with depth (see Box 1). (c) The penetration depth of the ion beam is well defined and can be varied by changing the ion energy. This is a unique characteristic which allows multi-level structures to be formed in one layer of resist. (d) Lithography with light ions offers a virtual absence of high energy secondary electrons which could otherwise give rise to unwanted exposure of resist (proximity effects). In e-beam writing for example, a small but significant fraction of secondary electrons

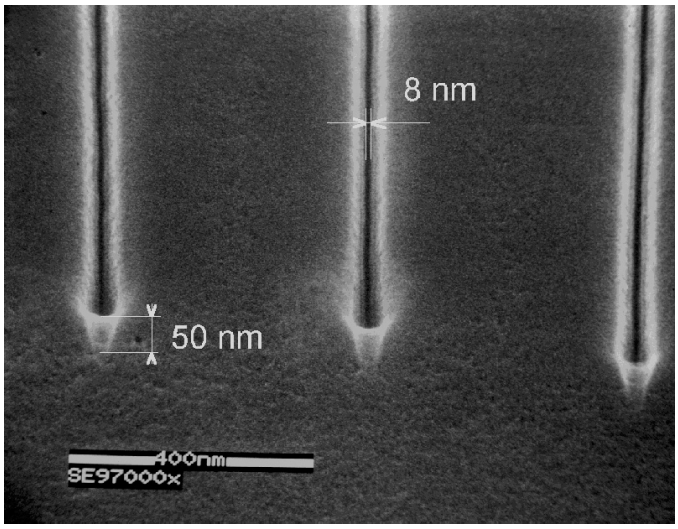

(a)

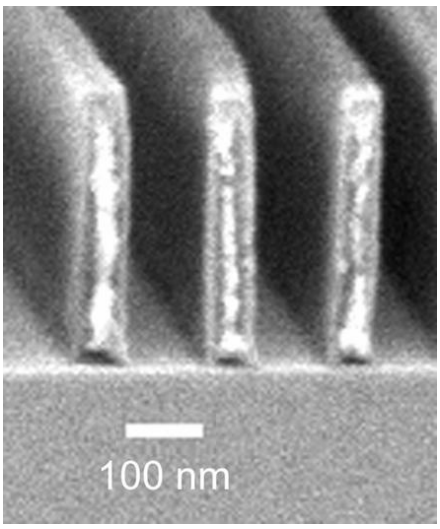

(b)

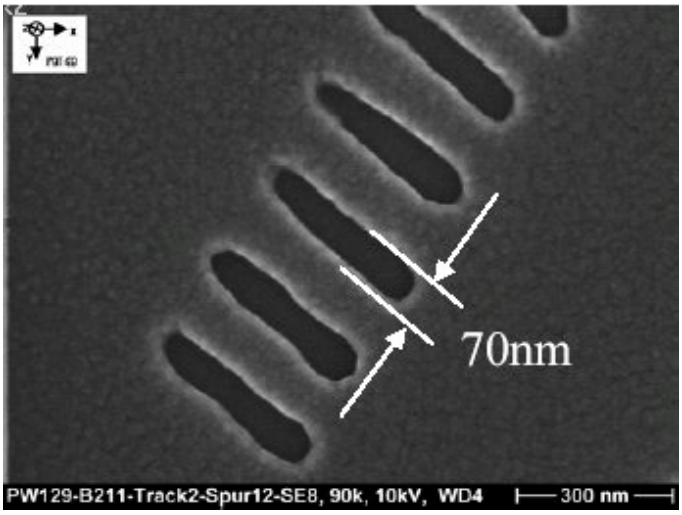

(c)

Fig. 4. Sub-100 nm ion beam fabricated structures: (a) 8 nm lines written into a multi layer sample of AlF3/GaAs using FIB,[6] (b) 50 nm walls fabricated in PMMA using *p*-beam writing with 2 MeV protons,[7] and (c) 70 nm slots fabricated in 50 nm Infineon resist using IPL operating with 45 keV He^+ ions.[8]

are generated with energies which can contribute to the proximity effect in the range of a few tenths of microns.

2. Ion Beam Techniques

2.1. *Focused ion beam (FIB)*

The FIB technique, the most mature of the ion beam nanolithographies, was developed in the late 1970s with instruments becoming commercially available

some 10 years later. FIB utilizes a direct-write focused beam of slow heavy ions (e.g., 30 keV Ga^+ ions), see Fig. 1, to sputter atoms or structurally modify the surface of a material to produce topographically or structurally modified surface patterns. A recent excellent review by Reyntjens and Puers outline the operating principles and application areas of FIB.[9] FIB is unique in that patterns can be produced in virtually any material, unlike other nanolithographies which are limited to patterning resist materials. Unfortunately, the process is relatively slow. For most materials, the material removal rate for a 30 keV gallium ion is around 1–10 atoms per incident ion, corresponding to a machining rate of around 0.1–1 μm^3 per nC of incident ions. By utilizing gas assisted etching (GAE) however, where the scanned area is simultaneously exposed to reactive gas molecules such as chlorine, the etching rate can be significantly enhanced.[10,11] More recently, FIB sputtering with poly-methylmethacrylate (PMMA) has produced a surface enhancement of the sputtering rate by several orders of magnitude.[12] A variation of FIB topographic patterning is 3D nanostructure fabrication using FIB chemical vapor deposition (CVD).[13–15] In FIBCVD, ambient gaseous molecules which are adsorbed on the surface are fragmented by the incident ion beam and deposited at the ion beam focus. The deposition rate is higher than for CVD using electrons, and the small penetration depth of heavy ions into the substrate allows complex high resolution 3D structures to be fabricated (e.g., see Figure (6b) and Refs. 13–15).

2.2. *Proton beam writing*

p-beam writing is a new technique that utilizes a focused beam of fast (MeV) protons written directly into a resist. The relatively high energy of the incident protons produces high penetration into the resist (e.g., a 2-MeV proton will penetrate 60 μm into PMMA). *p*-beam writing, pioneered at the Centre for Ion Beam Applications (CIBA), National University of Singapore, has the unique ability to direct write precise high-aspect-ratio 3D nanopatterns in conventional resists such as PMMA. When the resist is developed, material removal rates of around 10^6 μm^3 per nC of incident protons are observed, making the process up to one million times more efficient than conventional FIB for 3D patterning. Recent work has shown that *p*-beam writing is very effective in fabricating high aspect ratio and multi-level structures[7] (see also Figs. 5(b) and 6(c)) and also high aspect ratio structures in silicon, where the silicon is used as a negative resist material (see Fig. 7). A drawback of *p*-beam writing is that it is a new technology with no commercial instruments available as yet. Technical and commercial development has been hampered in the past by the difficulties encountered in focusing MeV ions to sub-100 nm dimensions. However, with the advent of compact magnetic quadrupole lens systems, these difficulties have recently been overcome[16] and the first prototype *p*-beam writer has recently been designed and constructed at CIBA.[7]

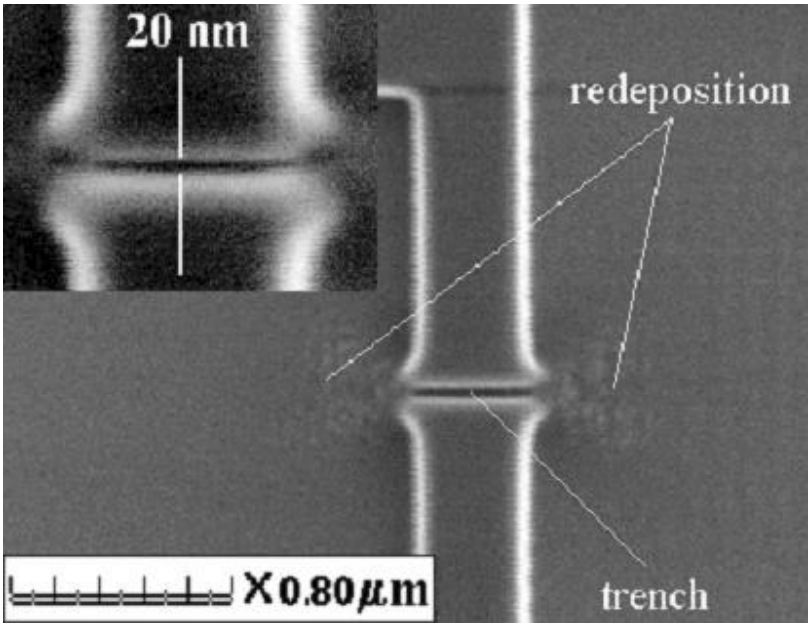

(a)

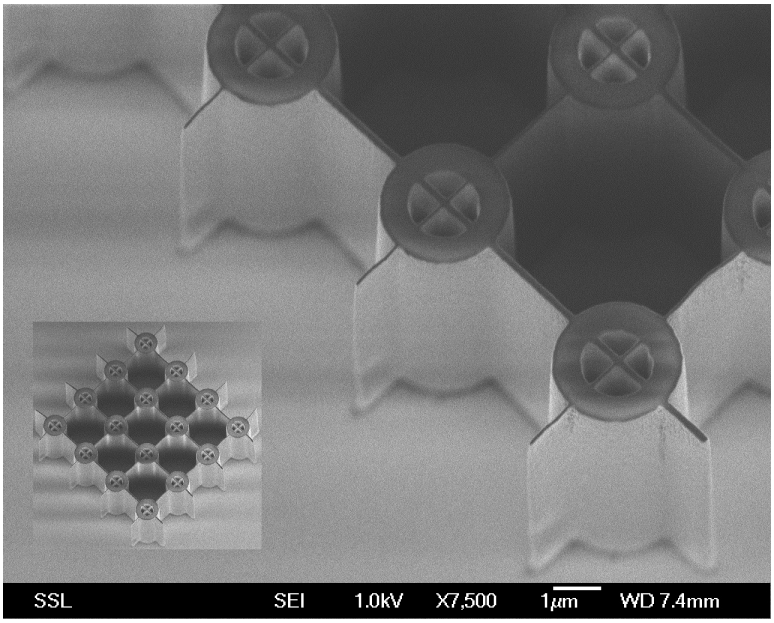

(b)

Fig. 5. High aspect ratio structures: (a) 20 nm trench (depth 400 nm) written in diamond using FIB[27] and (b) high-aspect-ratio test structures fabricated using *p*-beam writing in SU8 negative resist, showing 60 nm wall structures 10 micron deep.

2.3. *Ion Projection Lithography* (*IPL*)

The techniques of FIB and *p*-beam writing have distinct advantages over other lithographies for fabricating flexible and precise 3D nanostructures, but being direct-write techniques they lack the rapidity of fabrication for cost effective mass

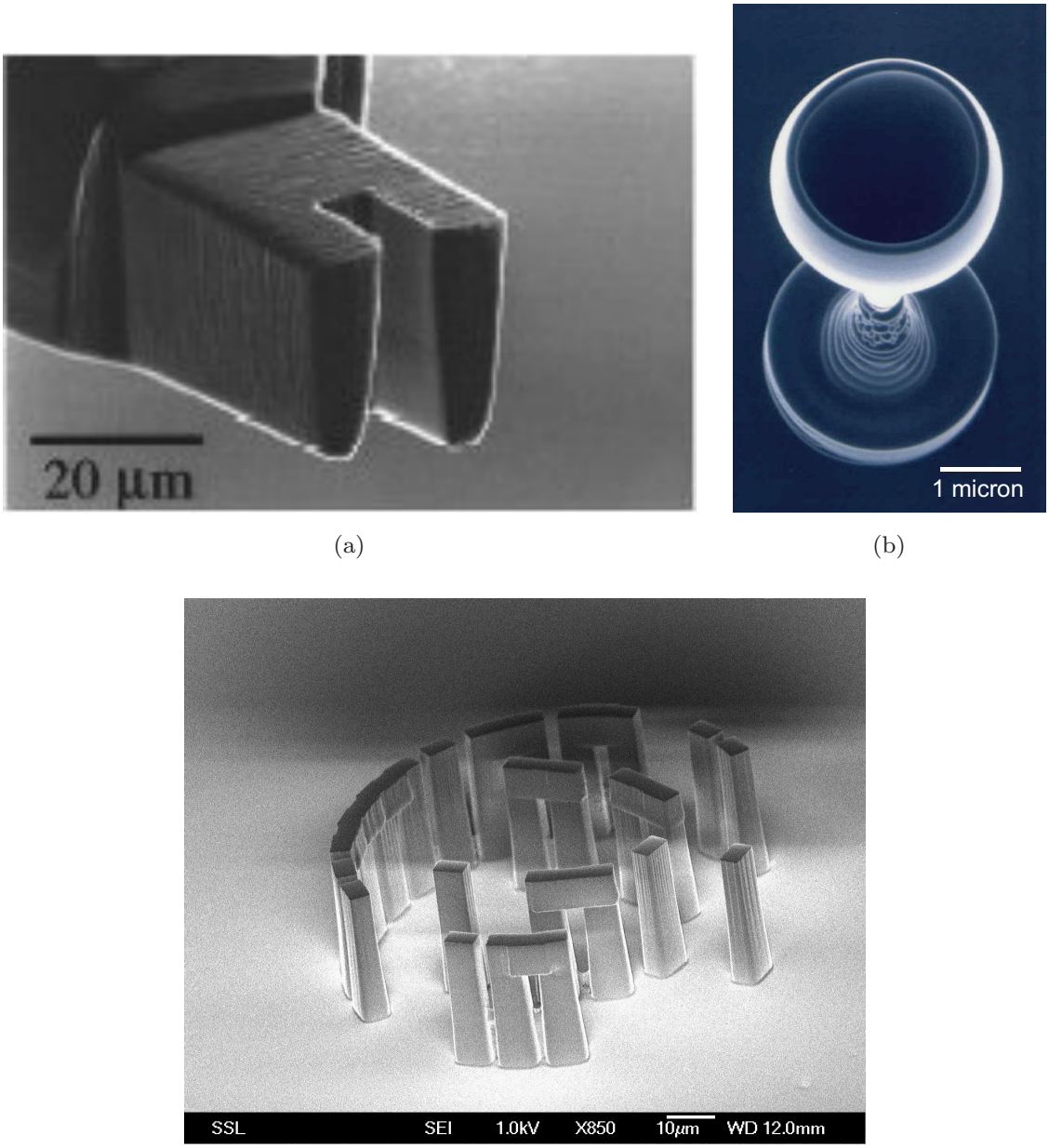

(a) (b)

(c)

Fig. 6. Complex shapes: (a) Custom made diamond tool fabricated using FIB sputtering,[58] (b) diamond like carbon micro-wine glass (2.75 micron external diameter and 12 micron height) fabricated using FIBCVD operating with 30 keV Ga and an aromatic hydrocarbon precursor.[13] (c) Micro-sized copy of the Stonehenge monument in the UK, fabricated using *p*-beam writing in SU8 resist (CIBA, Singapore). By utilizing the different depth exposure of two different proton energies: 500 keV for fabricating the horizontal slabs, and 2 MeV for exposing the vertical supports, the complete structure can be fabricated in one layer of resist.

production of components and devices compared with conventional masked lithography. Ion projection lithography (IPL)[17] utilizes medium energy (50–150 keV) ions (e.g., protons, H_2^+, He^+, Ar^+, etc.) and combines the bulk fabrication advantages of masked lithography with the unique properties of ions. IPL is pioneered at the Ion

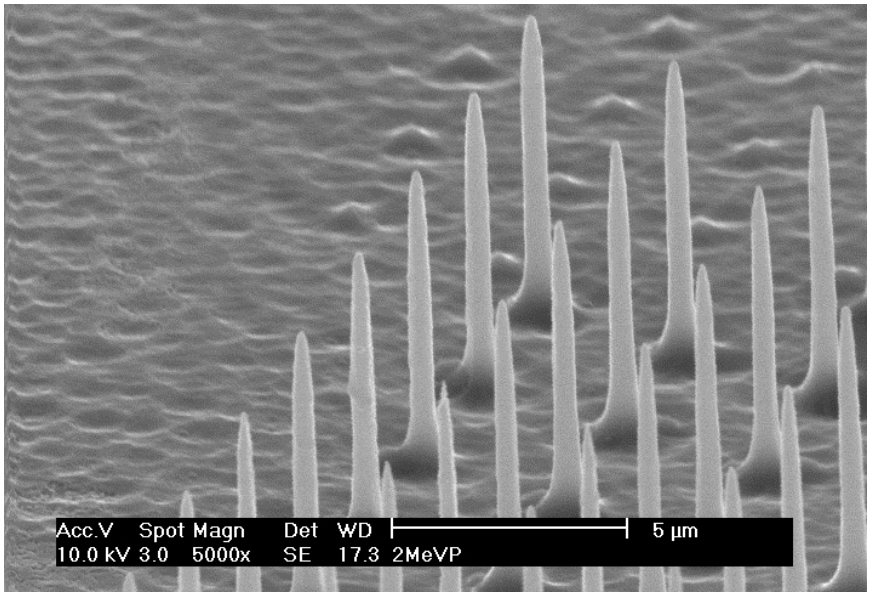

Fig. 7. An array of high aspect ratio silicon tips fabricated using *p*-beam writing (CIBA, Singapore). The silicon tips were fabricated by point irradiations with a 2-MeV proton beam, focused to a spot size of 200 nm, with a dose of $5 \times 10^{16}/\mathrm{cm}^2$. The proton beam induces damage along its track as it penetrates the silicon. The silicon is then subjected to electrochemical etching in hydrofluoric acid to produce porous silicon. However, the local production of porous silicon is retarded where the silicon is damaged, and subsequent removal of the porous silicon using KOH leaves behind silicon pillars several microns high, with tip radii of about 10 nm.

Microfabrication Systems GmbH (IMS) in Vienna. A beam of ions uniformly illuminates a large-area, robust, patterned stencil mask, and the transmitted beam is projected using electrostatic lenses, at an image reduction factor of one or two orders of magnitude, on to the workpiece surface. Working in a European consortium with combined expertise in ion projections optics,[8] stencil mask production,[18] and high contrast resist development,[19] IMS have succeeded in patterning at 50 nm resolution in parts of the exposure field, and 75 nm over the full field of 12.5×12.5 sq mm,[19] in a single beam exposure. The same group has also developed a variation to IPL which they call ion projection direct structuring (IPDS). Here, they use ions in order to modify the local magnetic anisotropy of the storage medium[20–23] thereby producing sub-100 nm bit patterns at extremely high densities[24] with no significant disturbance of surface topography, and no wet processing steps. For the future, the IMS design of a new generation PROjection Focused Ion multiBeam (PROFIB) tool with 200× reduction optics (Fig. 3) promises to be a powerful step forward in this technology.[25]

A further variation of IPL is the recently tested high energy (MeV) heavy ion projection system at Bochum in Germany.[26] Heavy ions (e.g., ^{28}Si and ^{12}C) are projected through a stencil mask onto a substrate to produce a patterned modification of the substrate through buried ion implantation. Even though this technology is relatively complex due to the problems involved in mask stability coupled with

producing and projecting heavy mass ions up to MeV energies, a creditable 300 nm resolution has been reached in initial tests.

3. Applications

The three ion beam processes are complementary and potentially cover a wide variety of application areas. The technical maturity and commercial availability of FIB has meant that the majority of ion beam applications to date have been carried out in this area. The distinctive feature of FIB is that it is capable of machining any material by surface erosion, and FIB has been widely applied to micro-technology and metrology, where great success has already been achieved in semiconductor failure analysis.[9] *p*-beam writing is much faster, and because of its deep penetration and straight trajectories into resist materials, is ideally suited for producing dimensionally accurate high aspect ratio 3D structures. However, with no commercial *p*-beam writing instruments yet available, the application areas have not been explored to the same extent as FIB. Both FIB and *p*-beam writing are eminently suitable for producing structures of high aspect ratio (Fig. 5) with a high degree of geometrical flexibility (Fig. 6), and being direct-write processes are very useful for rapid prototyping. IPL on the other hand is a masked process, and therefore is suitable for mass production, either for surface topographical patterning, or for nontopographic modification of the working material. Similar to *p*-beam writing, IPL is in its early developmental phase, and as such the application areas are mainly limited to performance testing and prototype structuring.

3.1. *Topographical patterning*

Much of the recent work so far on topographical patterning has been carried out by the well developed FIB technique, including patterning of diamond-like films,[27,28] and fabrication of nanoscale titanium honeycomb arrays.[29] FIB patterning coupled with *in-situ* etching,[30] fabrication of ordered nanochannels in alumina by growth guidance through FIB patterns,[31] carbon nanopillars grown by FIB assisted chemical vapor deposition (FIBCVD)[32] indicate the wide variety of applications in this area of nanotechnology. FIB has also been used in the fabrication of 3D stamps in silicon for micro-contact printing,[33–35] and micromolds and intricate 3D shapes in diamond-like-carbon have also been fabricated using FIBCVD.[13–15] Interesting applications using *p*-beam writing and FIB fabrication of micro and nanoscale 3D confinement environments for cells[36] and single molecule studies[37] have extended the use of topographical patterning into the biomedical field.

3.2. *Surface patterning through ion beam modification of surface properties*

In addition to surface sputtering, heavy ions such as Ga^+ can also cause atom intermixing and chemical disruption of the surface or subsurface. This effect can be

used to alter localized magnetic properties in a wide variety of magnetic materials for magnetic storage applications,[20–24,38–43] alter surfaces for self-assembled island nucleation through induction of defects,[44] produce oriented nanocrystals in amorphous alloys[45] and create ion induced localized surface amorphization.[46] Recent work using *p*-beam writing on carbon substrates has indicated that a high energy proton beam can also leave a trail of magnetic ordering due to hydrogen induced ferri-magnetism.[47]

3.3. *3D patterning for optical and micro-photonic applications*

The ability of FIB and *p*-beam writing to construct 3D structures of flexible geometry allows the rapid fabrication of micro-photonic components and systems. Both *p*-beam writing and FIB have been used to fabricate multiple lens arrays,[48–50] and waveguides of precise geometry coupled with low transmission loss[51] have been fabricated by *p*-beam writing using the negative resist SU8. Fabricating scaffolds of precise geometry for photonic band gap materials lends itself to techniques which can fabricate 3D structures in a precise manner, and both FIB and *p*-beam writing have the capability of fabricating these types of structures.[48,52–56] In particular, in an excellent demonstration of 3D micromachining (see Fig. 8), near infrared

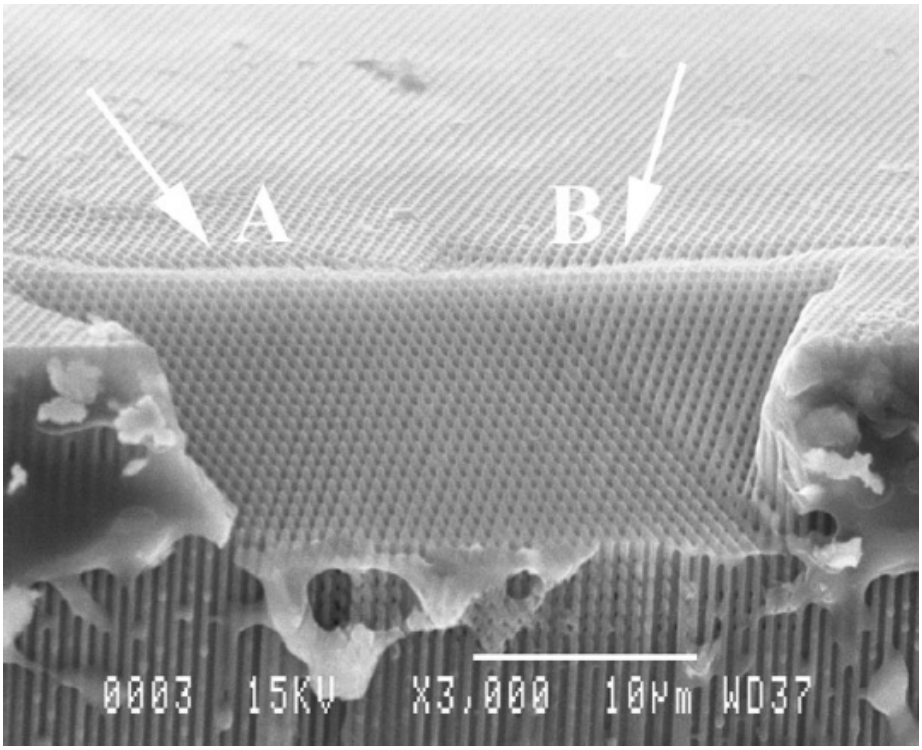

Fig. 8. Yablonovite-like crystal obtained by ion milling.[52] The milled surface corresponds to the (111) plane of the photonic crystal. The rectangular section on the sample side shows 25 periods in width and five periods in height. The FIB etching directions are indicated by arrows A and B. Some residual glue used for sample fixing can be seen on the sample sides.

three-dimensional Yablonovite-like photonic crystals have been fabricated using FIB etching of porous silicon.[52] Here potential problems of sputtered material clogging up machined channels are alleviated due to the dispersal of the sputtered material in the porous silicon pores, thereby leading to high aspect ratios. In a further recent development, the CIBA group in Singapore have extended their work on proton beam micromachining of semiconductors to studying patterned porous silicon.[53] Proton beam writing in silicon results in damage to the irradiated regions. During a subsequent electrochemical etch, the resulting porous silicon is formed at different rates and with different porosity in the damaged regions. Since porous silicon comprises an interconnected network of nanometer size silicon regions, the energy band gap within porous silicon is larger than that in bulk silicon owing to quantum confinement of the electron wavefunction, enabling the emission of visible light. The resultant photoluminescence intensity is proportional to the irradiated dose, being more intense where the dose is greatest. Figure 9 shows an example of

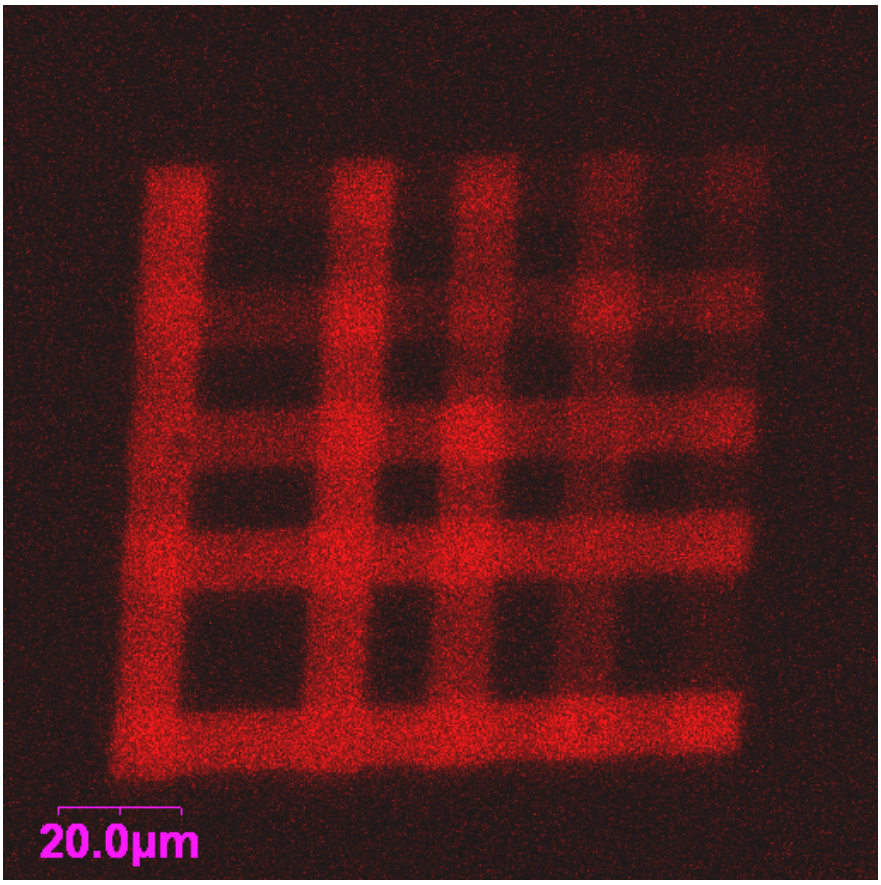

Fig. 9. Proton beam irradiation induced photoluminescence.[53] Photoluminescence (PL) image of a 0.02 Ohm.cm *p*-type silicon wafer which has been proton beam irradiated with different doses in a grid type pattern. Ion beam irradiation results in damage to the irradiated regions of the semiconductor, which results in porous silicon being formed at different rates and with different porosity when electrochemically etched. The resultant PL intensity is proportional to the irradiated dose, being more intense where the dose is greatest.

this proton-induced luminescence, where orthogonal lines have been irradiated with different proton doses, in a checkerboard pattern. For optoelectronic applications such as full-color display and optical interconnection, this process could provide tunable controlled light emission from adjacent, micron size areas of porous silicon with utilizable efficiency across the whole visible light range. Finally, the fabrication of high resolution diffractive optics[48,57–59] represents a growing interest in the application of ion beam fabrication techniques in the micro-photonics field.

3.4. *Rapid prototyping and one-off components*

As would be expected of the direct-write ion beam techniques where prefabricated masks are not required, the ability to rapidly fabricate prototypes is an area of high potential. FIB fabricated diamond and tungsten carbide microtools have been made in a variety of shapes that cannot be produced using conventional grinding and polishing techniques, e.g., microtools exhibiting triangular, rectangular or trapezoidal features.[60] These tools, which can be fabricated with dimensions in the 15–100 μm range, have been shown to have a radius of curvature cutting edge down to 40 nm (see for example Fig. 6(a)). Nanoscale planar superconductor–insulator–superconductor Josephson junctions[61,62] and a directly coupled superconducting quantum interference device (SQUID) magnetometer fabricated in magnesium diboride have been made using FIB.[63] In an interesting project involving the fabrication of devices for direct magnetic imaging, bismuth nano-Hall probes have been manufactured,[64] again using FIB. Other examples include the FIB fabrication of submicron cantilevers,[65] aperture probes for near-field optical microscopy,[66] and magnetic recording devices.[67]

In a new approach to producing high density storage devices, FIB has been used to nano-engrave a 2D array of defects in highly orientated pyrolitic graphite (HOPG). These defects, which can take the form of nanoholes or nanobumps, etc, can then act as traps for gold nanoclusters which have been preformed in the gas phase, thereby creating a high density pattern of quantum dots on the HOPG[68] compatible with TBit per cm^2 storage. Similarly, FIB implantation of micron-wide crossed *p*- and *n*-doped stripes into a pin-diode has resulted in good quality quantum dots being produced between the stripes, resulting in a micro-led array.[69]

A recent and a novel technique for the development of prototype quantum computers is the implantation of individual ^{31}P atoms in a solid matrix,[70,71] where various information extraction techniques have been proposed to address and manipulate the electrons and/or nuclear spins of adjacent implanted atoms.

4. Discussion and Outlook

FIB, *p*-beam writing and IPL can now attain sub-100 nm resolutions, and therefore must be serious contenders to play a major role in the next generation lithographies. The interesting feature of all these ion-based technologies is that diffraction problems are currently not an issue, and there is no fundamental diffraction limit

to hinder further development. For cheap and competitive mass production, IPL follows the traditional lines of lithography, utilizing large area masks through which a pattern is replicated in resist material or which are used to locally modify the near-surface properties. In IPL, the complete absence of diffraction effects coupled with ability to tailor the depth of ion penetration to suit the resist thickness or the depth of modification, are prime characteristics of this technique, as is the ability to pattern a large area in a single brief irradiation exposure without any wet processing steps.

One of Moore's corollaries to his now famous law suggests that the cost of manufacturing technology increases geometrically with time. The increased technical complexities and predicted increased cost of producing smaller feature sizes may call into question the traditional role of masked processes as the universal method of mass production. In particular, the advent of MEMS, nanophotonics, nanomagnetics, molecular nanotechnology devices and lab-on-a-chip systems, may benefit from radical new departures from established technologies. The direct-write processes, which for a long time have been considered too slow for mass production, may have some distinct advantages when used in combination with nanoimprinting.[31–34,72,73] Nanoimprinting technology (NIL) relies on the multiple transfer of a pattern into a substrate, and has high potential as a fast and cost effective solution of producing sub-100 nm features. This prime feature has been recognized in the latest International Technology Roadmap for Semiconductors 2003 Edition,[74] where imprint lithography has for the first time been added to the potential list of next generation lithographies, and direct-write techniques have been mentioned as possible avenues of high potential "*Direct-write lithography has been applied to niche applications in development and low volume ASIC production, but its role could be expanded. Breakthroughs in direct-write technologies that achieve high throughput will be a significant paradigm shift. It will eliminate the need for masks, offering inherent cost and cycle-time reduction*".

The success of nanoimprint lithography depends crucially on the quality of stamps that can be fabricated, and the use of ions have distinct advantages in this respect. FIB can produce master stamps in any material, and *p*-beam writing is ideal for producing high aspect ratio metallic stamps of precise geometry.[75] The transfer of large scale patterns using nanoimprinting represents a technique of high potential for the mass production of a new generation of high area, high density, low dimensional structures.

Finally, the unique properties of ions could also prove to be a useful adjunct to other developing lithographies. It is generally recognized that the development of conventional lithography below 100 nm requires improvements in mask technology. *p*-beam writing, which has the ability to construct sub-100 nm high aspect ratio structures, is ideally suited for advanced mask fabrication where relatively thick or robust masks are required (e.g., X-ray or Ion Beam Projection lithography). There is also an increasing interest in the use of STM/AFM tips for nanolithography, through the deposition and positioning of atoms or molecular clusters.[76] The flexibility of

p-beam writing for the fabrication of multiple tip assemblies in silicon for parallel writing could prove to be a very interesting development (Fig. 7).

In conclusion, the ion beam techniques FIB, *p*-beam writing, and IPL, offer a wide range of complementary techniques for the efficient production of sub-100 nm features and patterns. These techniques are in an ideal position to play a role in the next generation lithographies; IPL as a masked technique for bulk production, and FIB and *p*-beam writing as direct-write techniques with high potential for rapid prototyping and in the fabrication of precision stamps for nanoimprint lithography.

Acknowledgments

The authors wish to thank John Baglin, John Melngailis, Andrei Stanishevsky and Hans Loeschner, for valuable discussions and suggestions, and Jacques Gierak, Hans Loeschner, Andrei Stanishevsky, David Adams, Shinji Matsui, and Kang Wang for permission to use Figs. 4(a), 4(c), 5(a), 6(a), 6(b), and 8, respectively.

References

1. G. E. Moore, *Electronics* **38** (1965).
2. http://public.itrs.net. International semiconductor roadmap for semiconductors (2002).
3. J. F. Ziegler, *The Stopping and Range of Ions in Matter*, Vol. 2–6 (Pergamon Press, 1977–1985), http://www.srim.org/.
4. P. Hovington, D. Drouin, R. Gauvin, D. C. Joy and N. Evans, *Scanning* **19**, 29 (1997) http://www.gel.usherb.ca/casino/index.html.
5. Geant4: Low energy electromagnetic physics, http://www.ge.infn.it/geant4/lowE/index.html.
6. J. Gierak, A. Septier and C. Vieu, *Nucl. Instr. Meth. A* **427**, 91 (1999).
7. J. A. van Kan, A. A. Bettiol and F. Watt, *Appl. Phys. Lett.* **83**, 1629 (2003).
8. H. Loeschner *et al.*, *JM3 — SPIE J. Microlithography, Microfabrication and Microsystems* **2**, 34 (2003).
9. S. Reyntjens and R. Puers, *J. Micromech. Microeng.* **11**, 287 (2001).
10. R. J. Young, J. R. A. Cleaver and H. Ahmed, *J. Vac. Sci. Technol. B* **11**, 234 (1993).
11. I. Chyr and A. J. Steck, *J. Vac. Sci. Technol. B* **19**, 2547 (2001).
12. Y. Liu, D. M. Longo and R. Hull, *Appl. Phys. Lett.* **82**, 346 (2003).
13. S. Matsui, T. Kaito, J. Fujita, M. Komuro, K. Kanda and Y. Haruyama, *J. Vac. Sci. Technol. B* **18**, 3181 (2000).
14. T. Morita *et al.*, *Jpn. J. Appl. Phys.* **42**, 3974 (2003).
15. J. Fujita, M. Ishida, T. Ichihashi, Y. Ochiai, T. Kaito and S. Matsui, *Nucl. Instr. Meth. B* **206**, 472 (2003).
16. F. Watt, J. A. van Kan, I. Rajta, A. A. Bettiol, T. F. Choo, M. B. H. Breese and T. Osipowicz, *Nucl. Instr. Meth.* **210**, 14 (2003).
17. J. Melngailis, A. A. Mondelli, I. L. Berry and R. Mohondro, *J. Vac. Sci. Technol. B* **16**, 927 (1998).
18. R. Kaesmaier, A. Ehrmann and H. Loschner, *Microelectron. Eng.* **57–58**, 145 (2001).
19. S. Hirscher *et al.*, *Microelectron. Eng.* **61–62**, 301 (2002).
20. B. D. Terris, D. Weller, L. Folks, J. E. E. Baglin and A. J. Kellock, *J. Appl. Phys.* **87**, 7004 (2000).

21. C. T. Rettner, S. Anders, J. E. E. Baglin, T. Thomson and B. D. Terris, *Appl. Phys. Lett.* **80**, 279 (2002).
22. J. E. E. Baglin, B. D. Terris, D. K. Weller, J.-U. Thiele, A. J. Kellock, S. Anders and T. Thomson, *Proc. SPIE* **4468**, 1 (2001).
23. S. Maat, A. J. Kellock, D. Weller, J. E. E. Baglin and E. E. Fullerton, *J. Magn. Magn. Mater.* **263**, 1 (2003).
24. A. Dietzel *et al.*, *Adv. Mat.* **15**, 1152 (2003).
25. H. Loeschner *et al.*, *Proc. MRS: 3D Nano-Engineered Assemblies* **739**, 26 (2003).
26. U. Weidenmuller *et al.*, *J. Vac. Sci. Technol.* **20**, 246 (2002).
27. A. Stanishevsky, *Thin Solid Films* **398–399**, 560 (2001).
28. A. Stanishevsky, *Diamond and Related Materials* **8**, 1246 (1999).
29. H. Hosokawa *et al.*, *Mat. Sci. Eng. A* **344**, 365 (2003).
30. Y. Asaoka, T. Arai, N. Sano and T. Kaneko, *Compound Semiconductors 2001 Inst. Phys. Conf. Series* **170**, 331 (2002).
31. N. W. Liu, A. Datta, C. Y. Liu and Y. L. Wang, *Appl. Phys. Lett.* **82**, 1281 (2003).
32. M. Ishida, J. Fujita and Y. Ochiai, *J. Vac. Sci. Technol. B* **20**, 2784 (2002).
33. H.-W. Li, D.-J. Kang, M. G. Blamire and W. T. S. Huck, *Nanotechnology* **14**, 220 (2003).
34. R. Hull, T. Chraska, Y. Liu and D. Longo, *Mat. Sci. Eng. C* **19**, 383 (2002).
35. Y. Fu and K. A. B. Ngoi, *Optics Express* **10**, 436 (2002).
36. S. Feng, D. Casse, J. A. van Kan, R. Ge and F. Watt, *Tissue Eng.* **10**, 267 (2004).
37. E. Leclerc, Y. Mita and T. Fujii, *2nd Joint EMBS-BMES Conf. 2002*, Vols. 1–3, *Proc. Annual Int. Conf. IEEE Engineering in Medicine and Biology Society* (2002), pp. 1634–1635.
38. V. Nagarajan *et al.*, *Nature Mat.* **2**, 43 (2003).
39. S. Anders, *et al.*, *Microeoelectron. Eng.* **61**, 569 (2002).
40. R. Hyndman, *et al.*, *J. Magnetism and Magnetic Mat.* **240**, 50 (2002).
41. C.-M. Park and J. A. Bain, *IEEE Trans Magnetics* **38**, 2337 (2002).
42. T. Kimura, F. Wakaya and K. Gamo, *J. Vac. Sci. Technol. B* **20**, 2814 (2002).
43. M. Albrecht, C. T. Rettner, A. Moser, M. E. Best and B. D. Terris, *Appl. Phys. Lett.* **81**, 2875 (2002).
44. M. Kammler, R. Hull, M. C. Reuter and F. M. Ross, *Appl. Phys. Lett.* **82**, 1093 (2003).
45. R. Tarumi, K. Takashima and Y. Higo, *Appl. Phys. Lett.* **81**, 4610 (2002).
46. B. Basnar, *et al.*, *J. Vac. Sci. Technol. B* **21**, 927 (2003).
47. P. Esquinazi, D. Spemann, R. Hohne, A. Setzer, K.-H. Han and T. Butz, *Phys. Rev. Lett.* **91**, 227201 (2003).
48. A. A. Bettiol, T. C. Sum, C. H. Sow, J. A. van Kan and F. Watt, *Nucl. Instr. Meth. B* **210**, 250 (2003).
49. M. Kitamura, E. Koike, N. Takasu and T. Nishimura, *Jpn. J. Appl. Phys. — Part 1* **41**, 4019 (2002).
50. Y. Q. Fu and N. K. Bryan, *IEEE Trans. Semiconductor Manufacturing* **15**, 229 (2002).
51. T. C. Sum, A. A. Bettiol, J. A. van Kan and F. Watt, *Appl. Phys. Lett.* **83**, 1707 (2003).
52. K. Wang, A. Chelnokov, S. Rowson, P. Garoche and J.-M. Lourtioz, *J. Phys. D.* (*Appl. Phys.*) **33**, 119 (2000).
53. E. J. Teo, D. Mangaiyarkarasi, M. B. H. Breese, A. A. Bettiol and D. J. Blackwood, *Appl. Phys. Lett.* **85**, 4370 (2004).
54. M. Nakao *et al.*, *Optical and Quantum Electronics* **34**, 183 (2002).

55. K. Wang, P. Filloux, N. Paraire, P. Rocai Cabarrocas and P. Bulkin, *J. Vac. Sci. Technol. B* **21**, 966 (2003).
56. A. Chelnokov, K. Wang, S. Rowson, P. Garoche and J.-M. Lourtioz, *Appl. Phys. Lett.* **77**, 2943 (2000).
57. J. Cheng and A. J. Steckle, *IEEE J. Selected Topics in Quantum Electronics* **8**, 1323 (2002).
58. I. Chyr and A. J. Steckle, Focused ion beam machining of GaN photonic devices. *MRS Internet J. Nitride Semiconductor Res.* (1999) CODEN: MIJNF7.
59. M. Khan, G. Chantal, F. T. Hartley and J. Neogi, *Proc. SPIE* **3997**, 639 (2000).
60. Y. N. Picard, D. P. Adams, M. J. Vasile and M. B. Ritchey, *Precision Eng.* **27**, 59 (2003).
61. G. Burnell, R. H. Hadfield, C. Bell, D. J. Kang and M. G. Blamire, *Physica C* **372**, 14 (2002).
62. H. W. Seo, Q. Y. Chen, C. Wang, W. K. Chu, T. M. Chuang, S. F. Lee and Y. Liou, *Int. J. Mod. Phys. B* **15**, 3359 (2001).
63. G. Burnell, *et al.*, *Appl. Phys. Lett.* **81**, 102 (2002).
64. A. Sandhu, H. Masuda, K. Kurosawa, A. Oral and S. J. Bending, *Electron. Lett.* **37**, 1335 (2001).
65. J. McCarthy, Z. Pei, M. Becker and D. Atteridge, *Thin Solid Films* **385**, 146 (2000).
66. C. Lehrer, L. Frey, S. Petersen, T. Sulzbach, O. Ohlsson, T. Dziomba, H. U. Danzebrink and H. Ryssel, *Microelectron. Eng.* **57–58**, 721 (2001).
67. D. Litvinov and S. Khizroev, *Nanotechnology* **13**, 179 (2002).
68. A. Perez *et al.*, *New J. Phys.* **4**, article no. 76 (2002).
69. M. Vitzethum *et al.*, *Physica E* **13**, 143 (2002).
70. T. Schenkel *et al.*, *J. Vac. Sci. Technol. B* (2003), in press.
71. C. Yang *et al.*, *Nucl. Instr. Meth. B* **210**, 186 (2003).
72. Y. Xia and G. M. Whitesides, *Angew. Chem. Int. Ed.* **37**, 550 (1999).
73. R. F. Pease, *Nature* **417**, 802 (2002).
74. http://public.itrs.net/Files/2003ITRS/Home2003.htm.
75. K. Ansari, J. A. van Kan, A. A. Bettiol and F. Watt, *Appl. Phys. Lett.* **85**, 476 (2004).
76. R. D. Piner, J. Zhu, F. Xu, S. Hong and C. Mirkin, *Science* **283**, 661 (1999).